

This article was downloaded by:

On: 25 January 2011

Access details: *Access Details: Free Access*

Publisher *Taylor & Francis*

Informa Ltd Registered in England and Wales Registered Number: 1072954 Registered office: Mortimer House, 37-41 Mortimer Street, London W1T 3JH, UK



Journal of Liquid Chromatography & Related Technologies

Publication details, including instructions for authors and subscription information:

<http://www.informaworld.com/smpp/title~content=t713597273>

Imaging and Quantitation of One and Two Dimensional TLC With a New Radioanalytic Imaging System

Leonard A. Hook^a; Michael T. Macdonell^a; Alexis E. Traynor-kaplan^b

^a AMBIS Systems, Inc., San Diego, California ^b Department of Medicine, UCSD Medical Center, San Diego, California

To cite this Article Hook, Leonard A. , Macdonell, Michael T. and Traynor-kaplan, Alexis E.(1990) 'Imaging and Quantitation of One and Two Dimensional TLC With a New Radioanalytic Imaging System', *Journal of Liquid Chromatography & Related Technologies*, 13: 14, 2871 – 2899

To link to this Article: DOI: 10.1080/01483919008049075

URL: <http://dx.doi.org/10.1080/01483919008049075>

PLEASE SCROLL DOWN FOR ARTICLE

Full terms and conditions of use: <http://www.informaworld.com/terms-and-conditions-of-access.pdf>

This article may be used for research, teaching and private study purposes. Any substantial or systematic reproduction, re-distribution, re-selling, loan or sub-licensing, systematic supply or distribution in any form to anyone is expressly forbidden.

The publisher does not give any warranty express or implied or make any representation that the contents will be complete or accurate or up to date. The accuracy of any instructions, formulae and drug doses should be independently verified with primary sources. The publisher shall not be liable for any loss, actions, claims, proceedings, demand or costs or damages whatsoever or howsoever caused arising directly or indirectly in connection with or arising out of the use of this material.

IMAGING AND QUANTITATION OF ONE AND TWO DIMENSIONAL TLC WITH A NEW RADIOANALYTIC IMAGING SYSTEM

LEONARD A. HOOK^{1*},
MICHAEL T. MACDONELL¹,
AND ALEXIS E. TRAYNOR-KAPLAN²

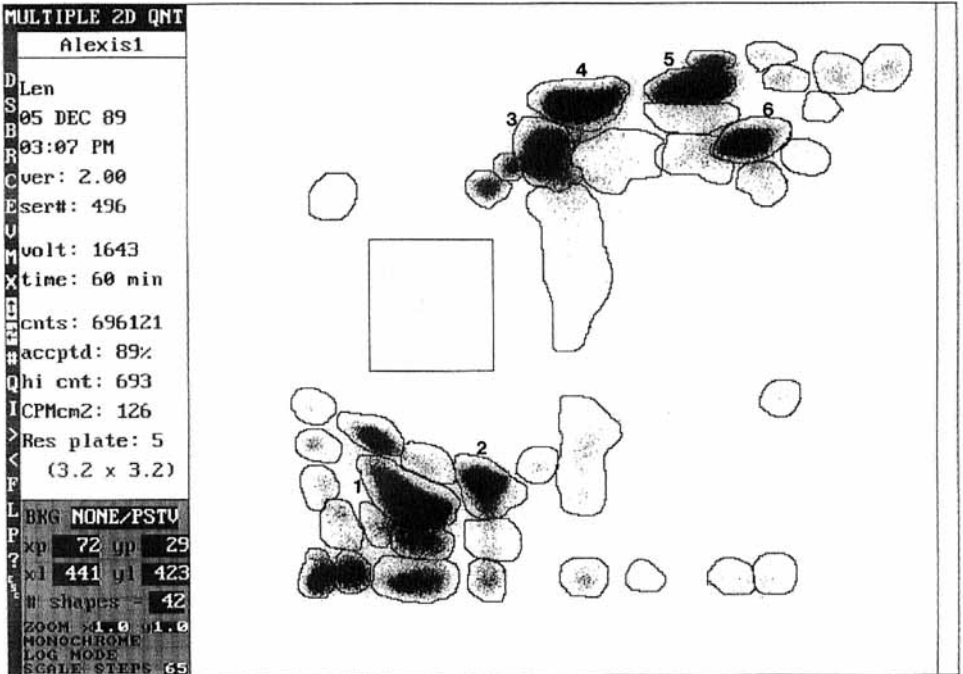
¹*AMBIS Systems, Inc.
3939 Ruffin Road
San Diego, California 92123*

²*Department of Medicine
UCSD Medical Center
225 Dickinson Street
San Diego, California 92103*

Abstract

A new method for the imaging and quantitation of radiolabeled substrates fractionated on one or two dimensional (2D) TLC plates has been developed. The TLC sample is read by a microcomputer-controlled beta- and gamma-sensitive gas proportional counter. The TLC plate is scanned by a 20 X 20 cm array of 952 individual detector elements, and the resulting quantitative image is displayed on a high resolution monitor for analysis. Individual radioactive spots may be quantitated on-screen.

* corresponding author



In the present study T_{84} cells were labeled with ^{32}P -orthophosphate, and stimulated with 10^{-4} M dioleoyl phosphatidic acid. The ^{32}P -labeled phospholipids were extracted separated in two dimensions by TLC. A 60 minute image acquisition at 3.2-mm resolution, of the stimulated cells, is shown below. The following major species were easily identified and quantitated [% of total activity]: (1) phosphatidyl inositol-4,5-bisphosphate ([^{32}P]PIP₂) [27.9%], (2) phosphatidyl inositol-4-phosphate [9.6%], (3) phosphatidyl inositol [23.4%], (4) phosphatidyl choline [13.1%], (5) phosphatidyl ethanolamine [10.5%], and (6) phosphatidic acid [4.0%].

Introduction

Planar Chromatographic Analysis. During the 1980s, radioanalytic imaging has gained acceptance in the scientific community as a standard method for the analysis of two-dimensional thin layer chromatography (TLC) plates. The system described herein is currently in use in more than 200 laboratories, worldwide. The central component of the system is a multiwire gas proportional counter which detects and quantitates radioactivity directly from the sample. The detector is able to image any flat sample of dimensions up to, and including, 20 X 20 X 1.0 cm, and provide linear quantitative data covering a range of nearly five orders of magnitude. Samples (wet or dry) commonly analyzed with this instrument include membranes (Southern, northern, and western blots), slot and dot blots, polyacrylamide or agarose gels, filters, and tissue sections. Although designed primarily for the analysis of beta-emitting isotopes, the detector is also sensitive to many gamma-emitters. The system is chiefly used for the analysis of ^{32}P , ^{14}C , ^{35}S , and ^{125}I .

Many laboratories routinely quantitate 2D TLC plates by first creating an analog image of the sample on x-ray film, a process typically involving several days. After imaging, the sample is then excised from the plate and counted by liquid scintillation. This method suffers from the necessity of lengthy imaging periods, and from the difficulty of quantitative removal of the radioactive materials from the plate. Furthermore, it is destructive of the sample. Radioanalytic imaging, on the other hand, allows rapid digital image acquisition and direct quantitation of radioactive spots with high resolution and precision.

The **AMBIS Radioanalytic Imaging System** is controlled by an AT-compatible microcomputer (either 386 or 286 CPU) through interactive, menu-driven software. Upon completion of data acquisition, the sample image is displayed on a high resolution (VGA-graphic) color monitor. The image may be enhanced in order to more easily identify the regions of interest for quantitation. Quantitation software allows the investigator to enclose the regions of interest in quantitation boxes. The quantitative data, R_f information, and the image, may be printed out on either a laser or color video thermographic printer.

Samples. Previous experiments with the T_{84} epithelial cell line have demonstrated that phosphatidic acid (PA) levels become elevated in these cells following stimulation with the agonists carbachol and histamine, agents which trigger Cl^- secretion. Both carbachol and histamine stimulate phospholipase C-mediated phosphoinositide hydrolysis and production of PA. Furthermore, addition of exogenous PA potentiates the effects of carbachol and histamine on Cl^- secretion as well as on calcium flux. This raises the question whether exogenous PA exerts its action on the same pathway as carbachol and histamine, or acts via an independent mechanism. The objective of this study was to determine the effect of added PA on phospholipid metabolism in T_{84} cells. This was measured most easily by 2D TLC.

One-dimensional TLC is frequently used in the molecular biology laboratory for performing the chloramphenicol acetyltransferase (CAT) assay. With this protocol, the investigator is measuring the enzymatic conversion of ^{14}C -chloramphenicol to acetylated ^{14}C -chloramphenicol. Prior to running the assay, a fusion gene is constructed in which the gene promoter under study is cloned

upstream from the CAT gene (Gilman, et al., 1986). The promoter, therefore, will direct the synthesis of a reporter protein (CAT enzyme) at a rate commensurate with its own degree of activity. The level of CAT enzyme production is proportional to the TLC-assayed rate at which chloramphenicol is converted to acetylated chloramphenicol.

In mammalian systems, control of cellular growth and differentiation depends, in part, upon the interaction of a number of messenger molecules which transduce signals from the outer cell surface through the cytoplasm to the nucleus. As part of this complex regulatory mechanism, the c-fos and c-jun oncogene promoters regulate the production of proteins which bind to cis-acting promoter elements and regulate transcription of certain target genes (Axel Schonthal, personal communication). The protein products of these (proto)oncogenes act as part of a regulatory mechanism controlling the activity of individual effector genes that produce metalloproteases and cysteine proteases. These, in turn, influence changes in the cell's phenotype from normal to cancerous. The ras gene product is a protein which is associated with the plasma membrane (inside the cell) and which is able to stimulate signal transduction pathways that are transmitted into the nucleus and activate the fos promoter. The objective of the CAT assay performed in this study was to investigate a signal transduction pathway by examining the effect of the presence of over-produced ras protein on the activity of the c-fos and c-jun promoters in mouse fibroblast cells.

Materials and Methods

Detector Design. The AMBIS detector is a modular instrument comprised of a head and base. The detector head, shown in cross-

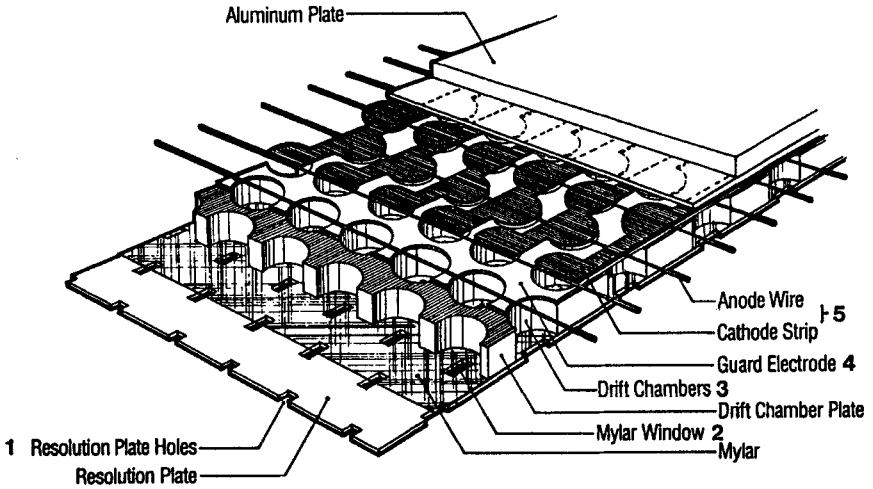


Figure 1. Cross-sectional diagram of the AMBIS detector. Beta particles enter the sensitive volume from below, passing through (in order): (1) resolution plate aperture, (2) 1.5- μ m thick mylar window, (3) drift chamber, (4) guard electrode, and (5) anode/cathode pair. (Nye, et al., 1988, figure reprinted, with permission, from American Biotechnology Laboratory, Vol. 6, no. 4, p. 18, 1988. Copyright 1988 by International Scientific Communications, Inc..

section in Figure 1, contains a hexagonal array of 952 individual detector elements. Each element is formed at the crossing point of one of 34 anode wires and 28 cathode strips. The instrument's base consists of a moving table which supports the sample. Using two high-precision stepping motors, the sample is carried through a series of programmed movements beneath the detector head. In this manner, the 952 detector elements are able to "see" all regions of the sample by scanning it.

Associated System Components. The standard computer used to operate the system is the **AST model 45, 386SX**. It operates at a clock speed of 16 MHz, and comes equipped with a 40 Mb hard drive, a 5.25 inch, 1.2 Mb floppy disk drive, and 1 Mb RAM. The AMBIS system may also be controlled with 286-type AT-compatible computers, such as the AST Premium 286, or the AST model 5, 386 CPU, operating at 33 MHz. Images are displayed via an extended 16-bit VGA graphics card on a **Sony CPD-1304** high resolution color monitor. Images and quantitative data are printed with the **Hewlett-Packard Laserjet Series II**, or the **Mitsubishi P75U** or **CP200U** video thermographic printers.

Software Design. AMBIS software is written in C language. It is menu-driven, and may be operated with a **MicrosoftTM** mouse or via the keyboard.

System Specifications. Resolution capabilities of the instrument were tested using two computer-aided-design (CAD) sources. These sources consisted of resolution lines, of known thickness and spacing, drawn with ^{14}C -spiked ink and a CAD plotter. The resolution samples were scanned for 2 h at resolution settings of 0.4 mm (vertical dimension) and 0.8 mm (both dimensions).

The counting linearity of the instrument was demonstrated by constructing a test source of known activity, and comparing the counts measured by the AMBIS instrument to those obtained from a liquid scintillation counter. A dilution series of spots containing increasing amounts of ^{14}C -labeled material was applied to a TLC plate and dried. The sample was scanned for 15 min. with the AMBIS instrument (3.2-mm resolution) and then the

radioactive spots were scraped from the plate and counted by liquid scintillation. Linearity was determined by plotting AMBIS cpm versus liquid scintillation cpm.

2D TLC: Phospholipid Metabolism. Two methods were used to test the effect of phosphatidic acid (PA) stimulation of T₈₄ cells: standard 20 X 20 cm TLC plates and high-performance (HP) TLC plates. The cells (an epithelial cell line derived from a human colon carcinoma) were labeled for 4 h with ³²P-orthophosphate, washed, and stimulated with 10⁻⁴ M dioleoyl phosphatidic acid. The ³²P-labeled phospholipids were extracted with chloroform-methanol-HCl and were separated in two dimensions by TLC. The organic phase was dried under nitrogen and resuspended in water-saturated chloroform. The first dimension was developed in chloroform-acetone-methanol-acetic acid-water (80:30:20:24:14) to the top of the plate. After overnight drying, the second dimension was developed in chloroform-methanol-concentrated ammonium hydroxide-water (90:90:7:22).

The 2D TLC plates were scanned for 60 minutes at 3.2-mm resolution. The samples' images were displayed with a logarithmic gray scale and the contrast (counts per pixel) was increased 30 - 70-fold in order to more clearly visualize the faintly labeled spots. After contrast enhancement, the samples were quantitated using the AMBIS **Multiple 2D Quantitation** software. Each radiolabeled spot was individually enclosed in a quantitation box, on-screen, with the aid of a computer mouse. Background counts were subtracted using the AMBIS **Baselevel Background Subtraction** feature. A region of each sample which was devoid of experimental activity was chosen to represent background. The activity in these areas was measured (cpm/cm²)

and automatically subtracted from the regions of interest on a "per unit area" basis.

1D TLC: the CAT Assay. The gene promoters under study, fos and jun, were cloned into a CAT reporter plasmid and co-transfected with the EJ(ras) expression vector into immortalized mouse fibroblast cells (NIH 3T3 cell line). This protocol forces the host cells to over-produce the ras protein for the purpose of studying its effect on the fos and jun promoters. Transfected cells were harvested and lysed by freeze/thaw cycling. Then the extracts were individually added to a Tris-buffered labeling cocktail containing [¹⁴C]chloramphenicol (92.5 kBq/mL), and acetyl-CoA. Each assay was incubated for 2 h at 37°C and then terminated by the addition of ethyl acetate. Fourteen samples (5 uL) were spotted onto the TLC plate and developed in 19:1 chloroform/methanol (vol/vol) for 2 h (Schonthal, 1990).

The CAT assay plate was scanned for 30 min. at 1.6-mm resolution. The image was displayed on the computer monitor using a logarithmic gray scale, followed by contrast-enhancement in order to highlight the weakly-labeled spots. Using the AMBIS Grid Quantitation software, the spots were quantitated lane-by-lane. Background counts were subtracted from the spots using the AMBIS Baselevel Background Subtraction feature. A region on the scan image that was devoid of experimental activity was chosen to represent background. The activity in this region was measured (cpm/cm²) and automatically subtracted from the spots on a "per unit area" basis.

Results and Discussion

Detector Function. The instrument is able to detect ionizing radiation through the principle of gas ionization. The

detector's sensitive volume is filled with a mixture of 90% argon and 10% methane (P-10 gas). Beta particles entering one of the 952 detector elements ionizes a number of Ar atoms, leaving a trail of free electrons along its track. These electrons are then accelerated within a drift chamber toward the anode wire, due in part to an electric field created by a small voltage on the guard electrode immediately above the drift chamber. The accelerated electrons interact with additional Ar atoms, causing an avalanche of ionizations in the vicinity of the anode wire. This process (gas amplification) generates a signal 1000 times greater than the initial ionizations. The electrons are collected by the anode wire, which operates at an electrical potential of 1250 V.

Software Function. The current core software, **ColorProbeTM** version 2.02, contains four menus: **Scan**, which operates the detector; **Image**, which generates the scan image on-screen and allows the user to quantitate and determine R_f values for regions of interest in a one or two dimensional mode; **Analyze**, which generates histograms from lane data and allows the user to quantitate peaks and obtain R_f data in a one dimensional mode; and **Utilities**, which contains AMBIS software housekeeping functions. The system software is multi-tasking, allowing the user to simultaneously operate one or two detectors while at the same time operating other software packages such as word-processors or spreadsheets.

Prior to entering a detector chamber, the ionizing particle must first pass through a collimating aperture in the resolution plate. As the name implies, the resolution plate apertures govern which areas of the sample are being "seen" at any given

time and determine the degree of resolution for the image. By adjusting the size of the resolution apertures, the user is able to select the degree of resolution needed for the sample. The integrity of the detector is maintained by the presence of a 1.5- μ m-thick mylar window placed between the resolution aperture and the opening of the drift chamber. This barrier prevents contaminating dust from entering the detector, and also assures the purity of the P-10 gas inside the sensitive volume by minimizing the diffusion of air into the detector.

The 34 parallel anode wires are arranged orthogonally to the 28 cathode strips, i.e., the anodes run north-south, and the cathodes run east-west. A beta particle entering the AMBIS detector generates a pulse of electrons collected by the anode/cathode pair. These signals are amplified and timed, such that a simultaneous appearance of signal from an anode/cathode pair identifies the point of origin of the event in the detector array. Thus, the position and number of each event is registered and stored by the computer. A schematic block diagram of the system circuitry is shown in Figure 2.

The pulse on the anode wire is fed to a dedicated high gain amplifier. After the anode pulse is amplified and inverted, it is sent to a comparator circuit where it is evaluated against a threshold voltage. The comparator signals are passed to the digital logic board for further processing. Signals originating on the cathodes are treated in a similar manner.

Mounted immediately above the detector array is the anti-coincidence detector. It is designed to intercept cosmic rays entering the detector which cause an elevated background count.

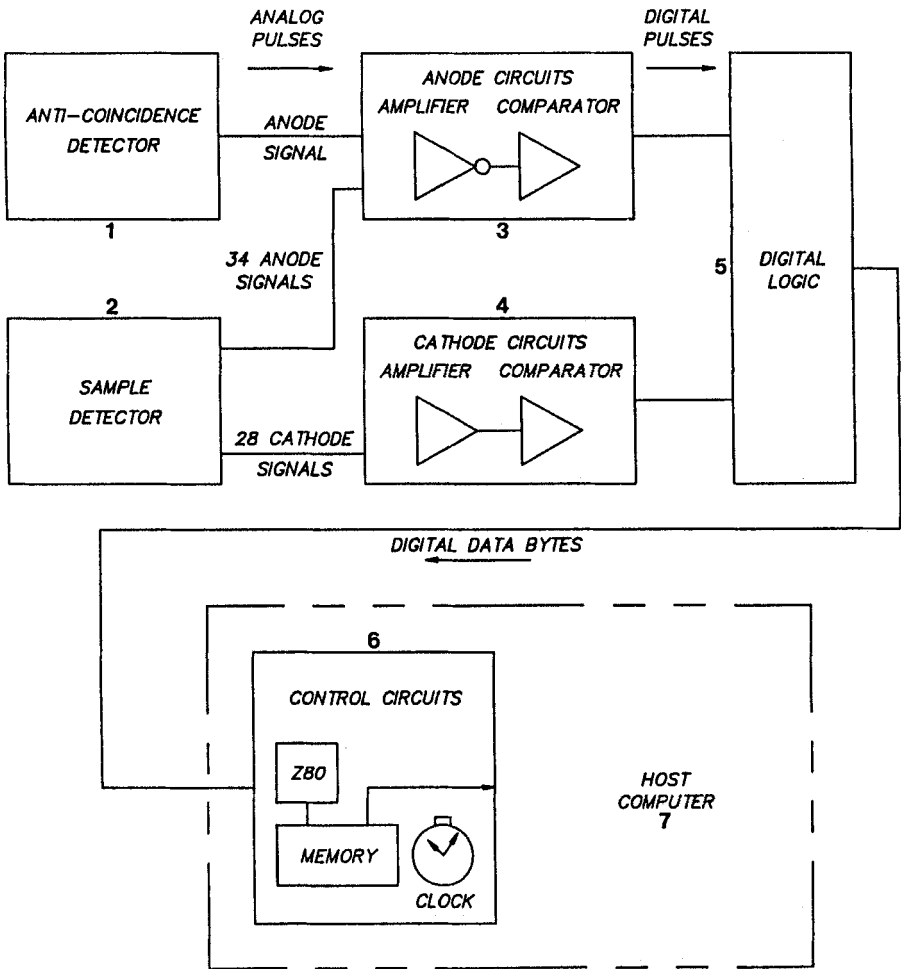


Figure 2. Circuit block diagram of the AMBIS detector. Signals are processed, in order, from the detectors, (1 and 2), through the amplifier boards, (3 and 4), to the digital logic board, (5), and finally to the control board, (6), inside the host computer (7).

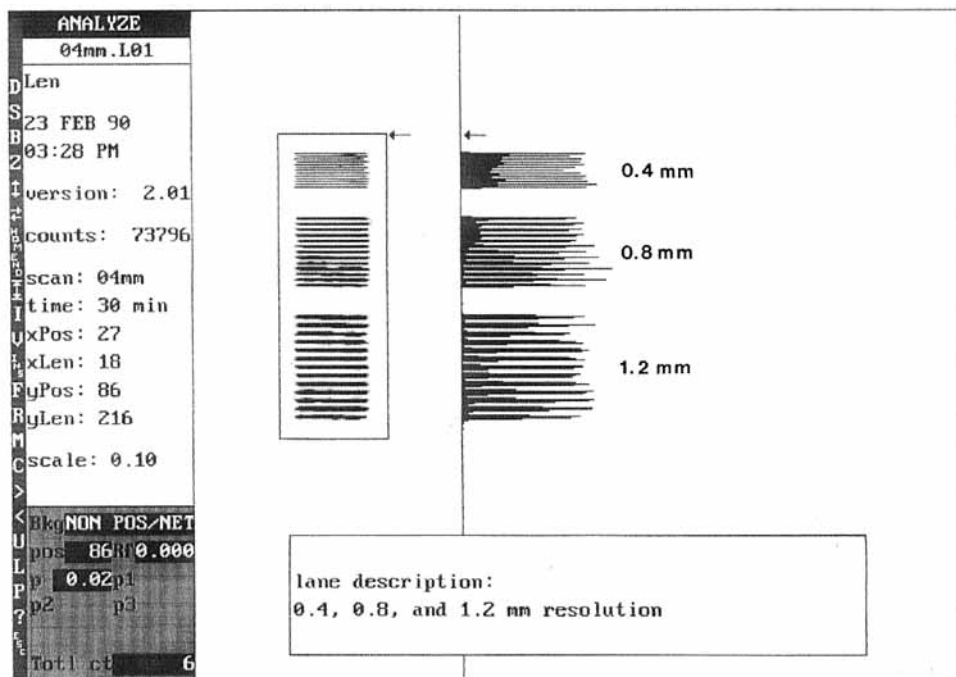


Figure 3. Resolution in one dimension (vertical) of 0.4-mm-spaced lines drawn by CAD plotter with ^{14}C -ink.

High energy cosmic rays are capable of activating the anti-coincidence detector and the sample detector simultaneously, making them easy to identify and reject. All of the comparator outputs from the anodes, cathodes, and the anti-coincidence detector are sent to the digital logic board, which examines the pulses, checks them for validity and encodes the data into 2 bytes. The data are then sent to the control board which registers the point of origin for each detected event.

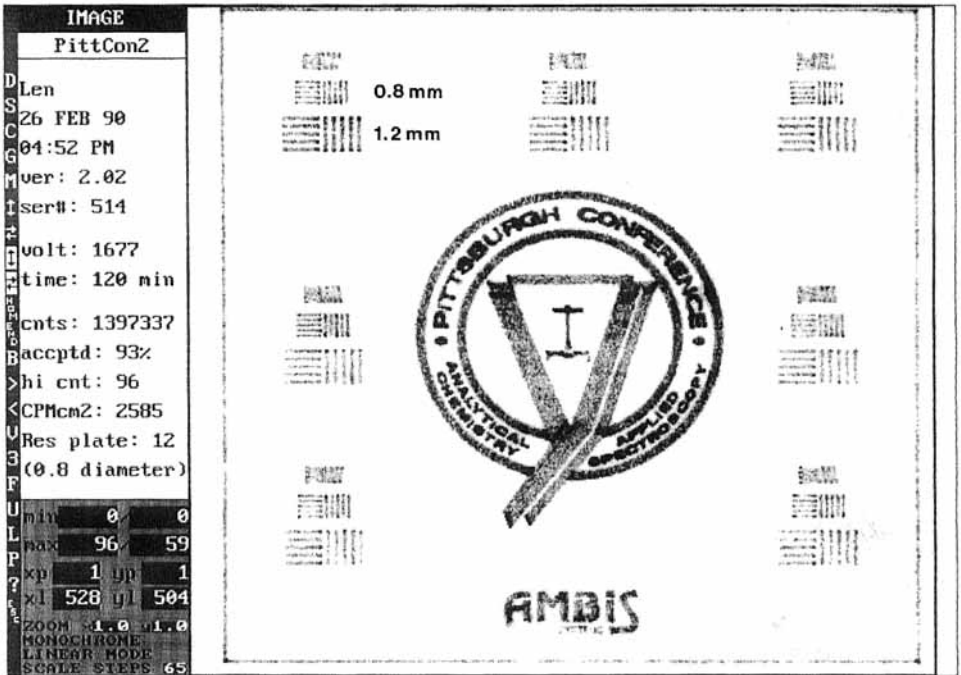


Figure 4. Resolution in two dimensions of 0.8-mm-spaced lines drawn by CAD plotter with ^{14}C -ink.

The control board is a Z80-based co-processor which resides in the host computer. In addition to performing its main function of off-line data collection, it also supervises the high voltage programming, sample table positioning, lifter actuation and control of gas flow. The control board maintains a software register (counter) for each of the 952 detector elements as well as a hardware timer to measure the length of time the sample is

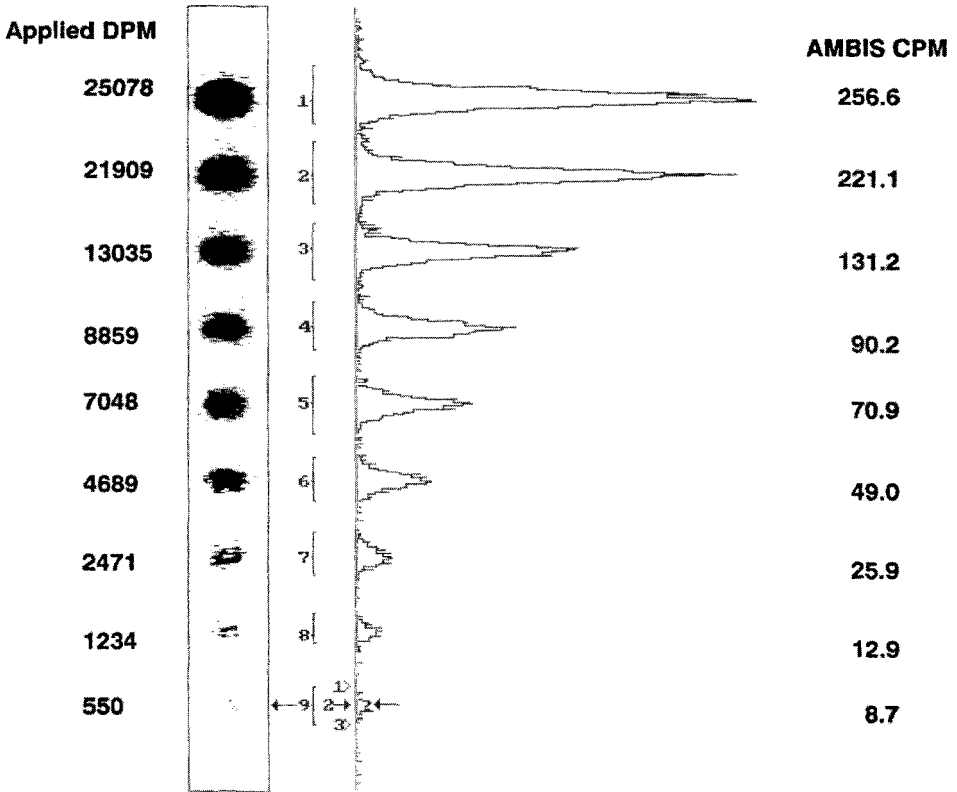


Figure 5. Histogram representation of ^{14}C dilution series spotted onto a TLC plate. The sample was scanned for 15 min. at 3.2-mm resolution. Applied dpm and AMBIS cpm are given for each spot.

held at each scanning position. At the end of each timed scan position, the control board halts the collection of data and alerts the host computer to take the data from memory and store it on the hard disk. The control board then indexes the sample to the next position, clears all software counters, and resumes data collection from 952 new positions.

Linear Regression Analysis

Correlation, $r = 0.99988$. Slope, $m = 0.010$

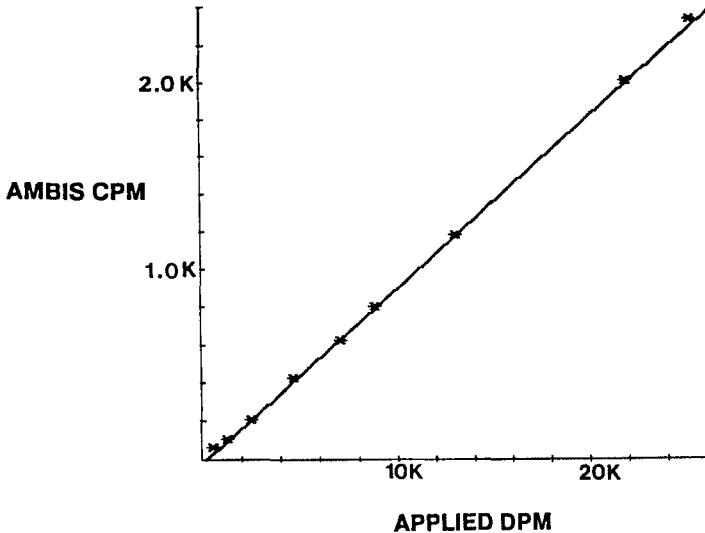


Figure 6. Applied dpm vs. AMBIS cpm. Linear regression analysis was performed on counts obtained from liquid scintillation (applied dpm) vs. AMBIS cpm. The plot shows linearity beyond 4 orders of magnitude.

Detector Resolution. Figures 3 and 4 illustrate the resolution capability of the detector based upon the resolving of CAD-drawn lines with ^{14}C -ink. The lines in Figure 3 were spaced, from top to bottom, 0.4, 0.8, and 1.2 mm apart. When the instrument was set for maximum resolution in the vertical dimension, the 0.4-mm lines were resolved below one-half peak height. When the instrument was set for equivalent resolution in two dimensions

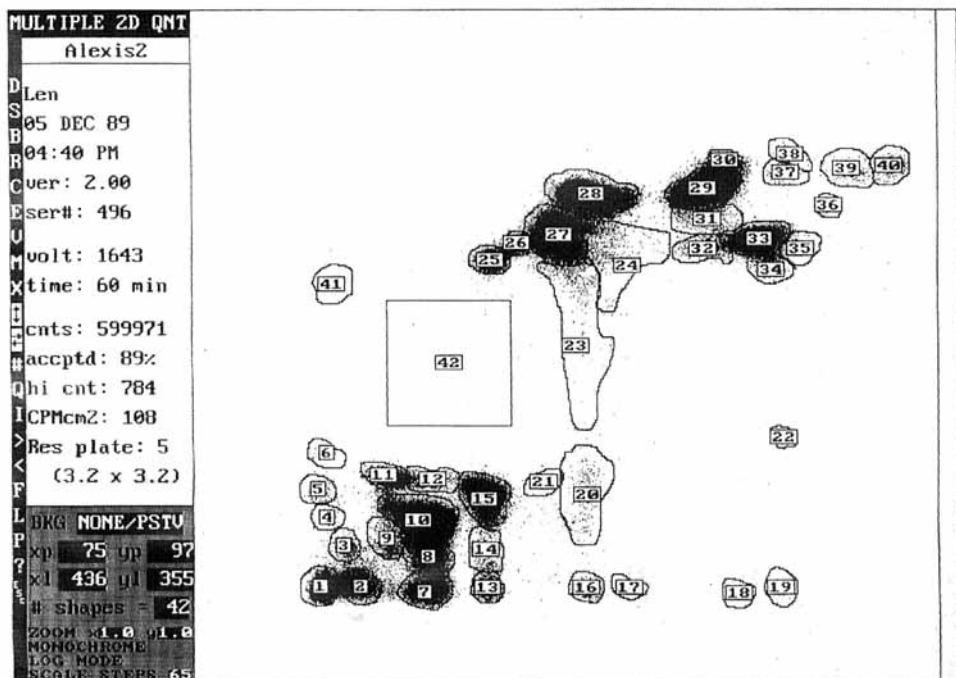


Figure 7. ^{32}P -phospholipids extracted from T_{84} cells. The spots were numbered sequentially, and the six major phospholipid species identified in Table 1.

(0.8 mm), the 0.8 mm-spaced lines were resolved to baseline (Figure 4).

A comparison of ^{14}C counts obtained with the AMBIS detector versus those obtained by liquid scintillation is shown in Figure 5. The lane image shows that a spot containing 550 applied dpm (bottom) was visible and quantitated in 15 min. scanning time.

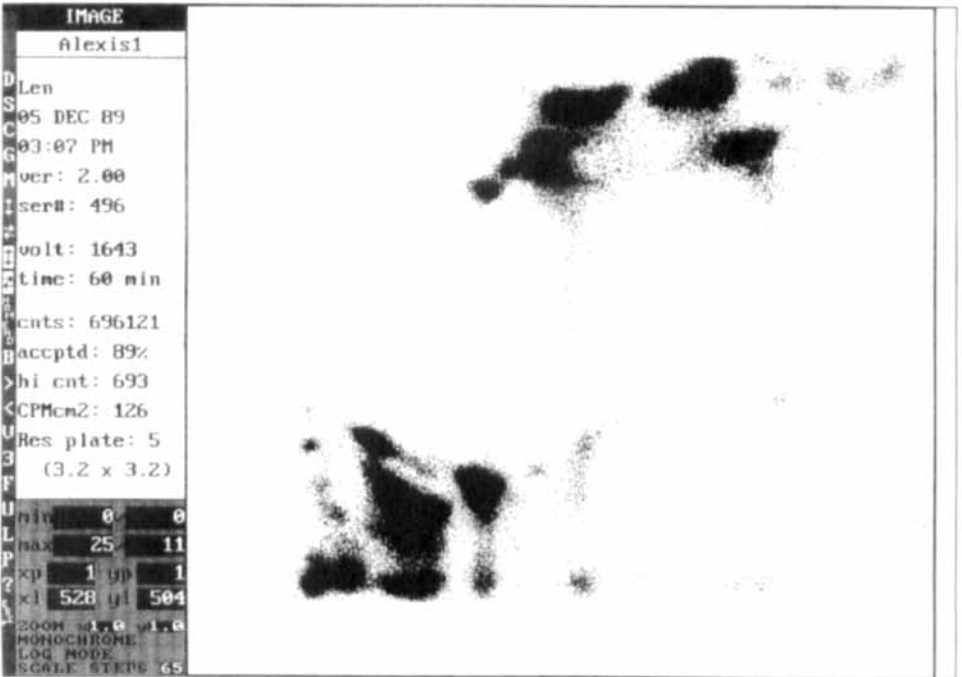


Figure 8. ^{32}P -phospholipids extracted from control T_{84} cells. Sample was scanned 60 min.

AMBIS cpm values were plotted against applied dpm and analyzed by linear regression analysis (Figure 6). The plot indicates linearity to 25,000 applied dpm. The slope of the plot, $m = 0.010$, gives the detector efficiency for ^{14}C when measured on a TLC plate (1.0%). Previous experiments have shown that 95 - 98% of ^{14}C betas are self-absorbed in the TLC matrix (data not shown).

Phospholipid Metabolism. The images of the plates testing the effect of phosphatidic acid stimulation of T_{84} cells are shown in

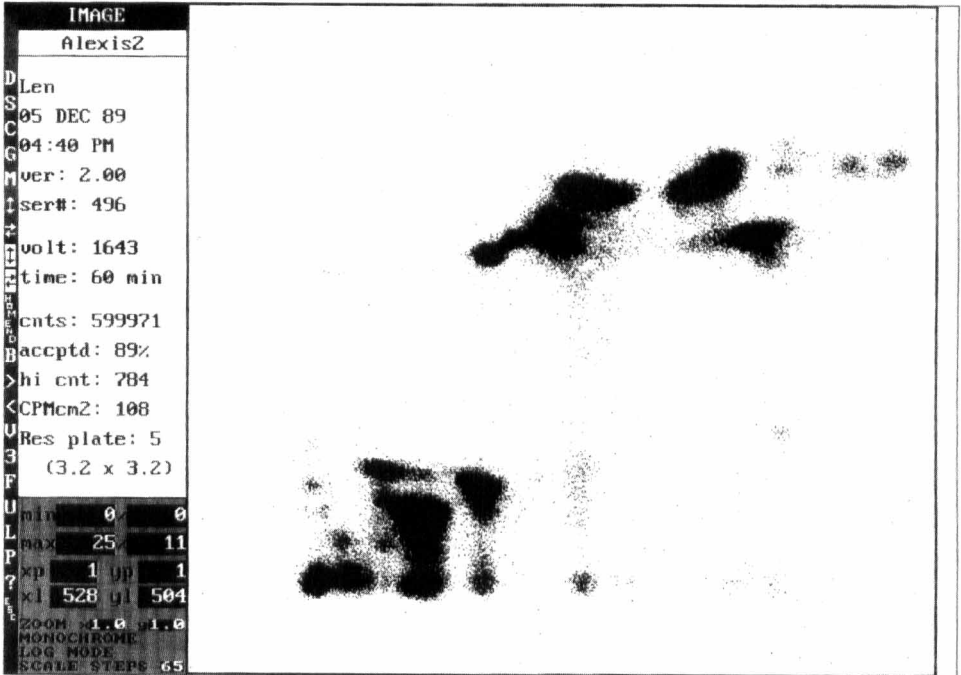


Figure 9. ^{32}P -phospholipids extracted from phosphatidic acid-stimulated T_{84} cells. Sample was scanned 60 min.

Figures 7 - 11 and 12 - 14. In the first experiment, standard 20 X 20 cm glass-backed TLC plates were used to compare phospholipid metabolism in control and stimulated cells. The control plate (Figures 7, 8 and 10), resolved six major phospholipid species listed in Table 1.

The same six major species were also identified in the stimulated cells (Figures 9 and 11). Numerous unidentified spots containing

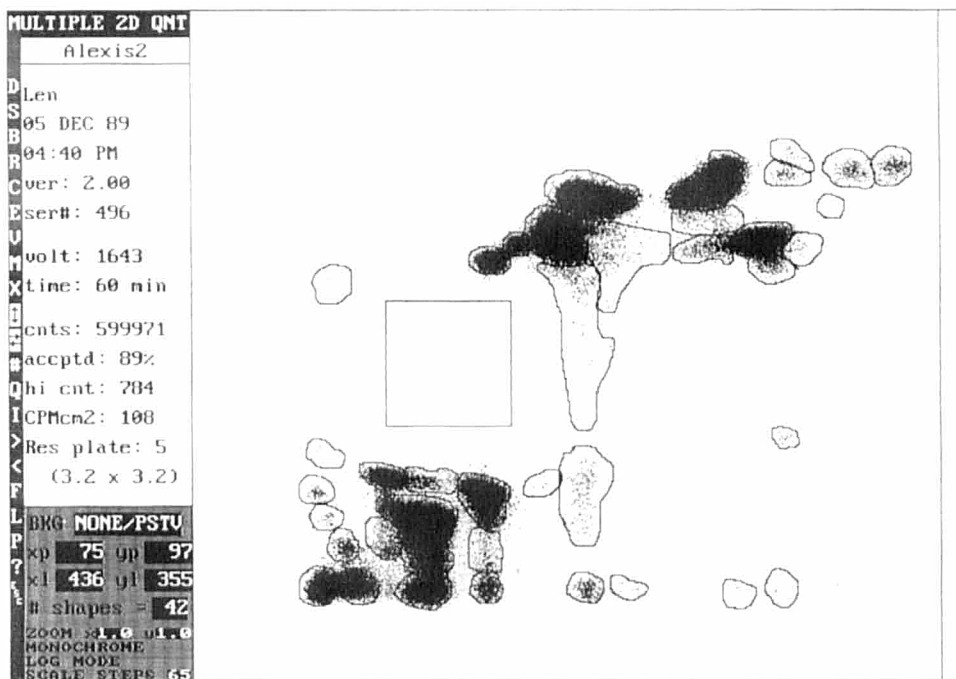


Figure 10. Control ^{32}P -phospholipids were identified and quantitated using AMBIS Multiple 2D Quantitation - Variable Shape software. The large square box was used to measure sample background (9.2 cpm/cm^2).

Table 1. Identification of six major phospholipids extracted from T_{84} cells. Refer to the designated spots in Figure 7.

<u>Spot No.</u>	<u>Metabolite</u>
7 - 10	phosphatidyl inositol-4,5-bisphosphate
13 - 15	phosphatidyl inositol-4-phosphate
27	phosphatidyl inositol
28	phosphatidyl choline
29	phosphatidyl ethanolamine
33	phosphatidic acid

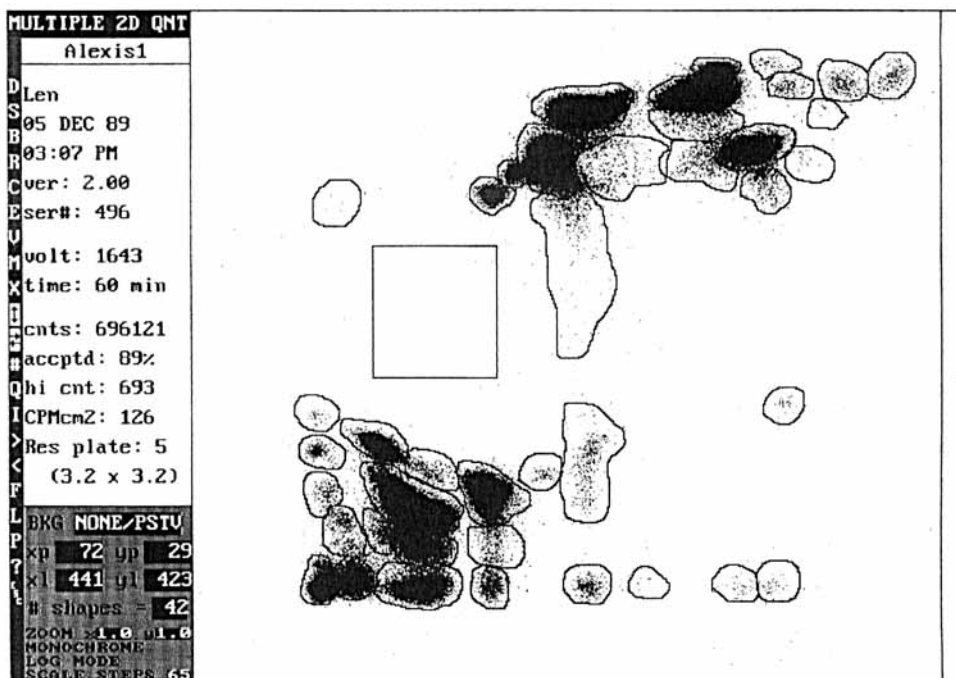


Figure 11. Stimulated ^{32}P -phospholipids were identified and quantitated using the AMBIS Multiple 2D Quantitation - Variable Shape software. The large square box was used to measure sample background (7.7 cpm/cm^2).

^{32}P were detected and quantitated, but these remain to be studied. Examination of the high-performance TLC plates (see Figures 12 - 14) indicated the presence of the same major species detected by standard 20 X 20 cm TLC. Some of the lesser (unidentified) metabolites were not resolved.

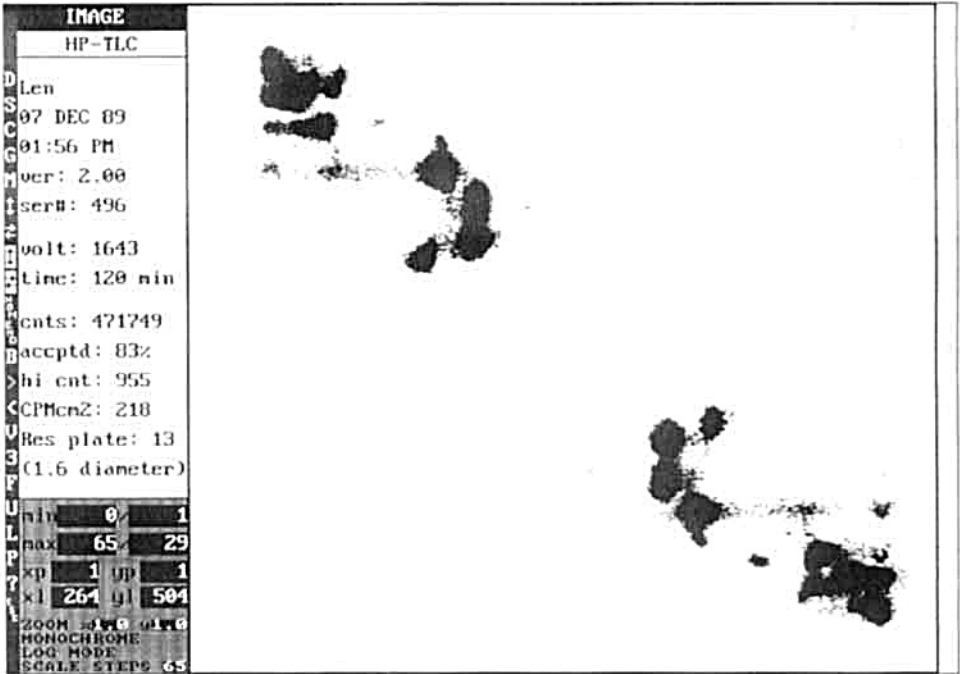


Figure 12. High Performance TLC: control T₈₄ cells (upper left plate) were extracted, and the ³²P-phospholipids were separated by 2D TLC. The plate in the lower right contained extract from T₈₄ cells stimulated with phosphatidic acid.

In order to normalize for differential total loading on each plate (stimulated and control), the data are presented as percentages of the total, as listed in Table 2, below.

The relative percentages of the major phospholipids assayed in each plate, whether by HP TLC or by standard TLC, appeared to be

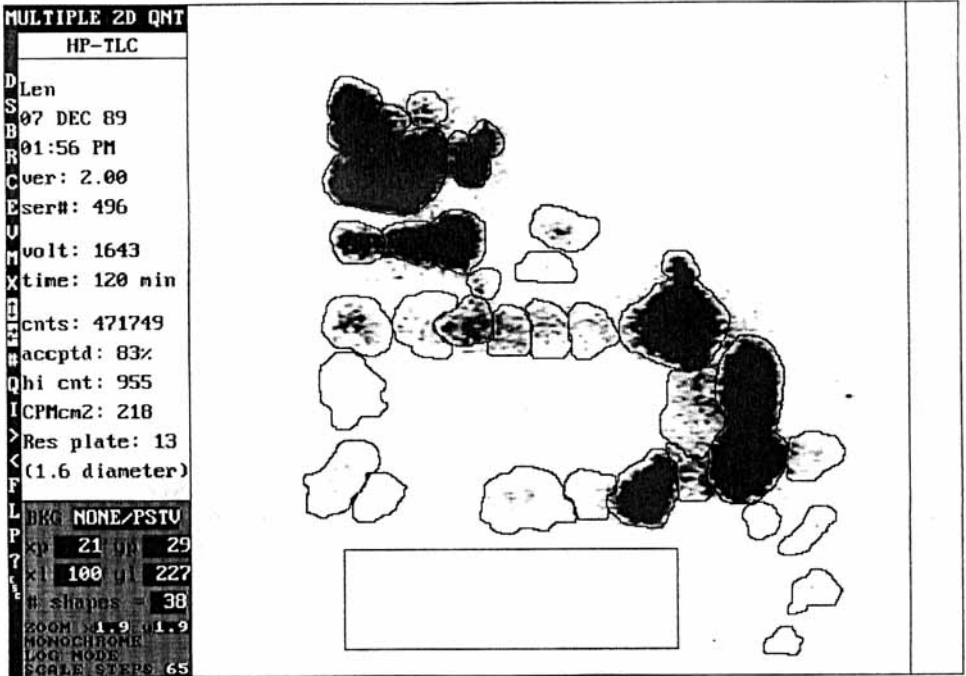


Figure 13. Enlargement from Figure 12, HP TLC separation of ³²P-phospholipids extracted from control T₈₄ cells. Radiolabeled spots were quantitated using the AMBIS Multiple 2D Quantitation software. The rectangle encloses the region selected to represent background, which measured 34.1 cpm/cm².

the same in the stimulated and control treatments. That is to say, one could not conclude from these data that stimulation of T₈₄ cells with phosphatidic acid had a notable effect on cellular phospholipid metabolism. The question of whether or not PA affects Cl⁻ release and Ca flux via the same mechanism as carbachol and histamine remains open.

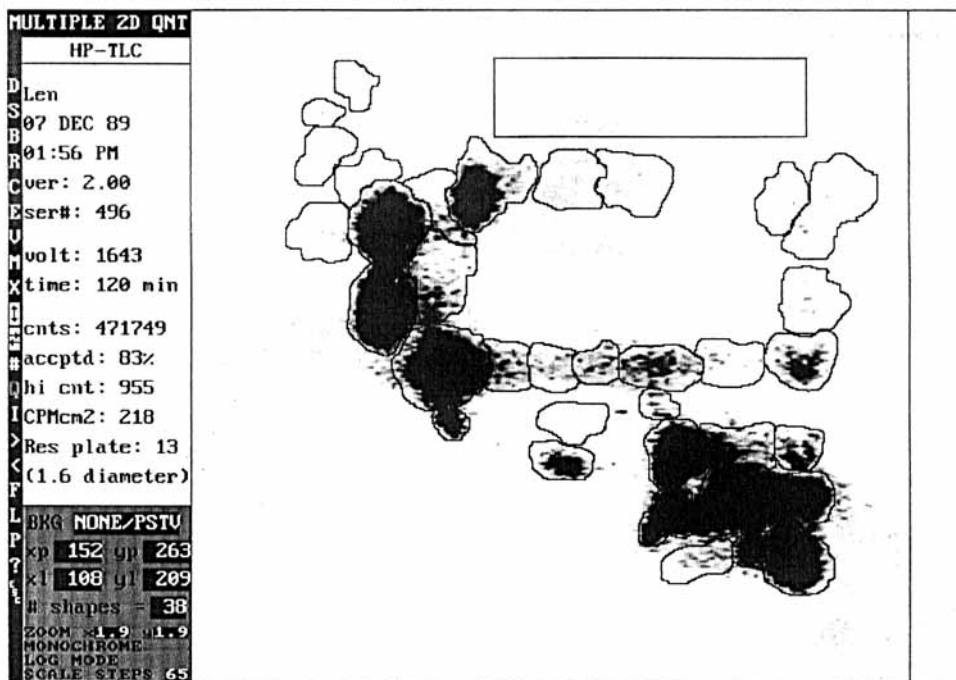


Figure 14. Enlargement from Figure 12, HP TLC separation of ^{32}P -phospholipids extracted from T_{84} cells stimulated with phosphatidic acid. Radiolabeled spots were quantitated using the AMBIS Multiple 2D Quantitation software. The rectangle encloses the region selected to represent background, which measured 34.5 cpm/cm².

CAT Assay. The contrast-enhanced printout of the 1-D TLC CAT assay is shown in Figure 15. Visible are 14 lanes of activity which are interpreted as follows. As shown in Figure 16, the spots were identified, in ascending order, as (a) origin, (b) unreacted

Table 2. Comparison of control and stimulated T₈₄ cell extracts from standard 20 X 20 cm. and high performance TLC plates.

Effect of Phosphatidic Acid (PA) Stimulation on Phospholipid Metabolism in T₈₄ Cells

<u>Metabolite</u>	<u>% of Total Counts</u>	
	<u>Control</u>	<u>Stimulated</u>
phosphatidyl inositol bisphosphate	27.0	27.9
phosphatidyl inositol phosphate	8.6	9.6
phosphatidyl inositol	24.3	23.4
phosphatidyl choline	13.5	13.1
phosphatidyl ethanolamine	10.2	10.5
phosphatidic acid	4.0	4.0
 <u>High Performance TLC</u>		
phosphatidyl inositol bisphosphate	29.2	28.2
phosphatidyl insitol phosphate	10.6	10.1
phosphatidyl inositol	20.5	22.3
phosphatidyl choline	14.1	14.7
phosphatidyl ethanolamine	8.6	11.2
phosphatidic acid	3.9	4.3

chloramphenicol, (c) and (d) acetylated chloramphenicol, and (e) diacetylated chloramphenicol (see Figure 16) (Ansubel, et al., 1987). The histograms shown in Figure 16 indicate relative activity in each lane (horizontal dimension) and composite activity in each spot (vertical dimension). The appearance of the diacetylated chloramphenicol spot in any given lane, or a

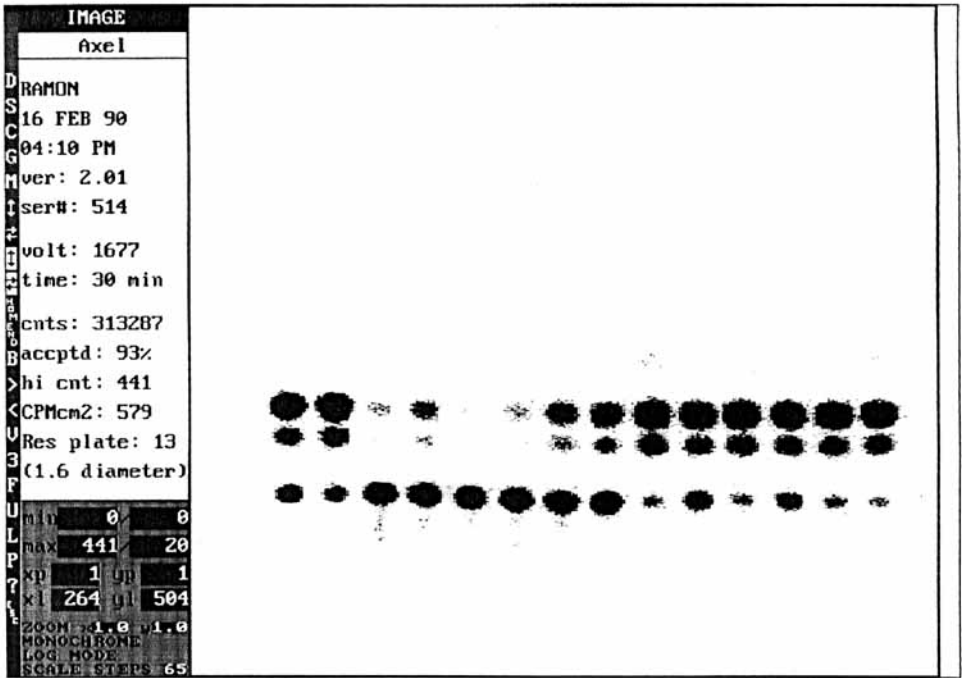


Figure 15. 1D TLC chloramphenicol acetyltransferase (CAT) assay. ^{14}C -chloramphenicol was enzymatically converted to acetylated ^{14}C -chloramphenicol.

conversion to monoacetylated chloramphenicol greater than 50-60%, is an indication that the assay mixture contained too much cell extract (protein), causing the assay to run beyond the linear range. The assay mixtures that fell within the linear range were analyzed by quantitating the percentage of counts found in the monoacetylated chloramphenicol spots versus the total activity in the lane.

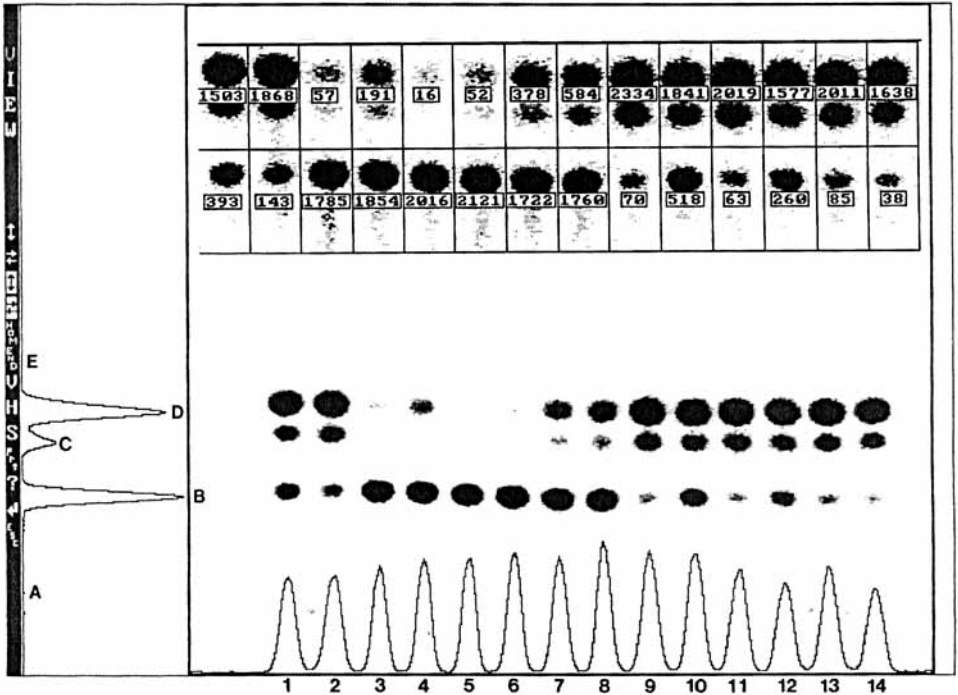


Figure 16. The histograms depict relative activity, lane-to-lane and spot to spot, of a 1D CAT assay. (A) origin (not visible), (B) unreacted chloramphenicol, (C) and (D) monoacetylated chloramphenicol, (E) diacetylated chloramphenicol (not visible). The enlarged portion at the top of the figure shows net counts contained in each quantitation enclosure.

The individual lanes were enclosed within a grid such that the monoacetylated species (upper boxes) were separated from the unreacted chloramphenicol (lower boxes, see Figures 16 and 17). Lanes 1, 2, and 9 - 14 all exhibited conversions of greater than 50%, indicating that the total protein content was too high and

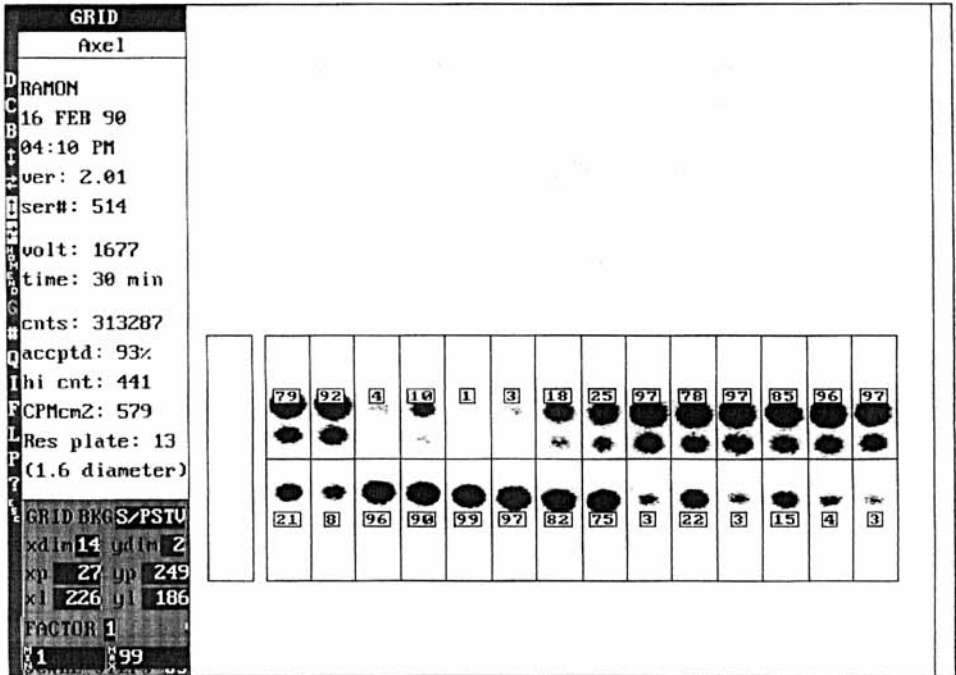


Figure 17. Conversion of ^{14}C -chloramphenicol (lower row of boxes) to acetylated ^{14}C -chloramphenicol (upper row of boxes). The values displayed in each box are a percentage of the activity in each lane. The box at the extreme left was selected to represent background (34.3 cpm/cm²).

caused the reactions to run beyond their linear range. As shown in Figure 16, the presence of over-produced ras protein (lane 4) activates the fos promoter 3.3-fold compared to the treatment without over-produced ras protein (lane 3). Lanes 7 and 8 (controls) show that the promoter of SV-40 is only weakly induced (18% vs. 24% conversion) by ras protein (Schonthal, 1990).

Acknowledgments: We thank Axel Schonthal for generously providing the CAT assay data, William Truchan and John Colclough for AUTOCAD drawings and descriptions of circuit design, and Darlene Munoz and Larry Wolfen for assistance with graphics. Thanks are also extended to Robert Harrison and Phillip Kinningham for a critical review of the manuscript. For further information, contact AMBIS Systems, Inc., 3939 Ruffin Rd., San Diego, CA 92123, (800) 882-6247 or (619) 571-0113, FAX (619) 571-5940.

Literature Cited

Gilman, M.Z., Wilson, R.N., and Weinberg, R.A. 1986. Multiple protein-binding sites in the 5'-flanking region regulate c-fos expression. *Mol. Cell. Biol.* **6**:4305-4316.

Schonthal, A. 1990. Nuclear protooncogene products: fine-tuned components of signal transduction pathways. Manuscript in preparation, personal communication.

Ansubel, F.M., et al. (eds). 1987. *Current protocols in molecular biology*. Greene Publishing Assoc. and Wiley-Interscience, New York.

Nye, L., Colclough, J.M., Johnson, B.J., and Harrison, R.M. 1988. Radioanalytic imaging: high speed radioisotope detection, imaging, and quantitation. *Amer. Biotech. Lab.* May 1988.